JOURNAL OF SOLID STATE CHEMISTRY 21, 79–90 (1977)

Crystal Structure, Mössbauer, and Magnetic Behavior of Mixed Valence Compounds in the Ba–Fe–S System: $Ba_3(Ba_{1-x}Al_x)Fe_2S_6[S_{1-y}(S_2)_y]$

J. T. HOGGINS, L. E. RENDON-DIAZMIRON, AND H. STEINFINK

Materials Science Laboratories, Materials Science and Engineering Program, The University of Texas at Austin, Austin, Texas 78712

Received October 15, 1976; in revised form December 29, 1976

The compounds $Ba_4Fe_2S_6[S_{2/3}(S_2)_{1/3}]$ and $Ba_{3.6}Al_{0.4}Fe_2S_6[S_{0.6}(S_2)_{0.4}]$, designated I and II, were prepared by reacting BaS, Fe, and S powders and Al foils in graphite containers sealed in evacuated quartz ampoules at approximately 1100°C. The crystal structure of I was determined using 1682 independent, nonzero X-ray reflections, while 3589 were used for II. They are triclinic, $A\bar{1}$:

$a = 9.002(2)$ Å, $b = 6.7086(8)$ Å, $c = 24.658(4)$ Å, $\alpha = 91.49(2)°$,
$\beta = 105.10(2)°$, $\gamma = 90.74(2)°$, $\rho_{calc} = 4.15$ g/cm^3, for I:
$a = 8.993(6)$ Å, $b = 6.780(7)$ Å, $c = 24.70(1)$ Å, $\alpha = 91.11(6)°$,
$\beta = 105.04(6)°$, $\gamma = 90.90(9)°$, $\rho_{calc} = 3.90$ for II.

BaS_6 trigonal prisms share edges to form distorted hexagonal rings which form one-dimensional chains leaving two free lateral edges. The chains link in a stairstep manner with the rings offset along the [301] direction. These stairsteps join in a complicated manner to form a three-dimensional network. Fe ions are in two sites forming isolated FeS_4 tetrahedra and isolated Fe_2S_6 dimers by edge-sharing tetrahedra. The Al substitution occurs in the trigonal prisms which have free edges with Al replacing Ba.

Room-temperature Mössbauer isomer shifts are 0.20 mm/sec. for I and 0.30 mm/sec for II. These data indicate that upon Al substitution charge compensation occurs by reducing Fe^{3+}. Valence calculations indicate that Fe in edge-sharing tetrahedra are reduced while the Fe in the isolated tetrahedron remains unchanged. The effective charge distribution in the Al substituted compound is approximately Fe^{3+}, $Fe^{2.5+}$ with electron delocalization across the shared edge. Room temperature electrical resistivity is 10^5 ohm/cm.

The compositions of the crystals are best represented by the formulas $[Ba_4Fe_2S_7]_{2/3} \cdot [Ba_4Fe_2S_6(S_2)]_{1/3}$ and $[Ba_3AlFe_2S_7]_{0.4} \cdot [Ba_4Fe_2S_7]_{0.2} \cdot [Ba_4Fe_2S_6(S_2)]_{0.4}$. The replacement of a sulfide by a disulfide ion is thought to be strongly dependent on the sulfur activity during the preparation.

Introduction

The investigation of the barium–iron–sulfur system has revealed a large number of compounds with complex stoichiometries in which iron displays mixed as well as single-valued valence states and only S^{2-} ions are present [*1–4*]. In a continuing investigation we have synthesized and characterized a new phase, which resulted from an attempt to substitute Al in the compound $Ba_7Fe_6S_{14}$ (*1*) to form the solid solution series $Ba_7(Fe_{6-x}Al_x)S_{14}$, $x \leqslant 2$. It was expected that the determination of the Al position replacing Fe would yield information regarding the oxidation states of iron in this mixed valence compound. However, the Al did not substitute for Fe but a new phase was formed in which Al replaced Ba. Charge balance is maintained by reduction of the Fe ion. Subsequently, this same phase without Al was synthesized. We report here the structural determinations

ISSN 0022-4596

as well as results of the Mössbauer and magnetic measurements.

Experimental

The compounds were prepared by reacting powders of BaS, Fe, and S and microtomed Al foils, so that nominal stoichiometries of the mixtures were $Ba_7Al_2Fe_4S_{14}$ and $Ba_8Fe_4S_{14}$. Extra sulfur to the extent of 10% of the total sample weight was added to the reaction mixture. The mixtures were placed into graphite containers, sealed in evacuated Vycor glass tubing and heated between 1050 and 1200°C for 3 days.

Mössbauer spectra were obtained using a constant acceleration drive operated in the time mode. Data were accumulated in a 400-channel analyzer. The source was 20 mCi of ^{57}Co diffused into palladium foil and used at room temperature. Velocity calibration was obtained using a laser interferometer (*5*). The absorbers consisted of a finely ground powder with a thickness of approximately 150 mg/in.^{2}. The data were corrected for parabolic motion effects, and the spectra were fitted by least-squares analysis assuming Lorentzian line shapes and using a modified National Bureau of Standards program. The reproducibility for values of line positions is generally ±0.02 mm/sec or better.

The measurements of magnetic susceptibility as a function of temperature were carried out on a Faraday balance which was calibrated with $Hg[Co(CNS)_4]$. The possible influence of ferromagnetic impurities on the susceptibility data was eliminated as described in Ref. (*6*).

Chemical quantitative analyses of single crystals selected from the reaction mixture were obtained using a scanning electron microscope operated at 25 keV with a non-dispersive X-ray spectrometer attachment. Peak heights and background counts were measured on the unknowns and standards and used in the computer program MAGIC IV (by J. W. Colby at Bell Laboratories). The results in atom percent were: Ba, 28.2, 30.7; Al, 4.1; Fe, 15.1, 16.1; S, 52.1, 53.1; the first values refer to the Al-containing phase and the second values to the Al-free phase. The relative error for this procedure is approximately 7%.

Data Collection

$Ba_3(Ba_{1-x}Al_x)Fe_2S_6[S_{1-y}(S_2)_y]$

Weissenberg and precession photographs of numerous crystals selected from the reaction products showed that they were always twinned. The diffraction symmetry appeared to be $2/m$ with systematic absences hkl, $h+k=2n+1$ consistent with the space groups Cm, $C2$, $C2/m$. The lattice constants from film measurements were $a=24.6$ Å, $b=6.75$ Å, $c=8.89$ Å, and $\beta=105.0°$. The twinned crystal, a parallelepiped with approximate angles of 83°, 97°, and 90° measuring approximately 0.10 mm on each edge, was mounted parallel to the b^* axis and placed on an automated diffractometer having the Weissenberg geometry and equipped with a graphite monochromator. During the collection of three-dimensional intensity data, it was discovered that the b^* axis was not perpendicular to the a^*c^* plane, thus indicating that the above space group was incorrect and instead was $C1$ or $C\bar{1}$; $P1$ or $P\bar{1}$ in the conventional orientation. The positions of 55 reflections with 2θ between 23° and 67° were carefully measured using Mo$K\alpha$ radiation ($\lambda=0.71069$ Å) and a 0.5° receiving aperture. The reflections from the twins superimposed exactly for $(h0l)$ and were completely separate for hkl, $k \geq 4$. The reflections used in the lattice constant determination were from this set. The 2θ measurements, made at room temperature, were used in a least-squares refinement for the determination of the constants. The previously designated a and c axes were interchanged to maintain a right-handed system. The results are shown in Table I. The A-centered cell will be maintained since it shows the pseudo-symmetry and twinning more clearly. The lattice constants for the A-centered cell give an angle of 1.43° between b and b^*. The transformation matrices are given by:

$$\begin{bmatrix} h \\ k \\ l \end{bmatrix}_A = \begin{bmatrix} 1 & 0 & 0 \\ 0 & 1 & 0 \\ 0 & 1 & 2 \end{bmatrix} \begin{bmatrix} h \\ k \\ l \end{bmatrix}_P$$

TABLE I

CRYSTALLOGRAPHIC DATA FOR THE TWO COMPOUNDS[a]

	$Ba_4Fe_2S_6[S_{2/3}(S_2)_{1/3}]$		$Ba_3(Ba_{0.6}Al_{0.4})Fe_2S_6[S_{0.6}(S_2)_{0.4}]$	
	P	*A*	*P*	*A*
a	9.002 (2)	9.002 (2) Å	8.993 (6)	8.993 (6) Å
b	6.7086 (8)	6.7086 (8) Å	6.780 (7)	6.780 (7) Å
c	12.861 (2)	24.658 (4) Å	12.869 (7)	24.70 (1) Å
α	106.61 (1)°	91.49 (2)°	106.38 (6)°	91.11 (6)°
β	104.27 (2)°	105.10 (2)°	104.17 (6)°	105.04 (6)°
γ	90.74 (2)°	90.74 (2)°	90.90 (9)°	90.90 (8)°
z	2	4	2	4
ρ_{calc}	4.15 g/cc		3.90 g/cc	

[a] The estimated standard deviation given in parentheses refers to the last decimal place.

and

$$\begin{bmatrix} x \\ y \\ z \end{bmatrix}_A = \begin{bmatrix} 1 & 0 & 0 \\ 0 & 1 & 0 \\ 0 & -\frac{1}{2} & \frac{1}{2} \end{bmatrix} \begin{bmatrix} x \\ y \\ z \end{bmatrix}_P$$

For the collection of the diffraction intensities the crystal was now aligned along the *b* axis of one of the twins. Intensities from layers *h*1*l* and *h*2*l* were not recorded since the reflections overlapped, and the method of scanning would not allow both peaks to be recorded together. In layer *h*4*l* the separation was great enough to resolve the reflections. In layer *h*3*l* the reflections were not well resolved, so this layer was not used in the refinement but only in some Fourier synthesis calculations of electron density maps. Data within each level were collected to $(\sin\theta)/\lambda = 0.867$ using an ω scan. The detailed procedure is described by Lemley *et al.* (*3*). A total of 4369 independent reflections was measured in layers $k = 0$, 4–9, of which 3589 were considered observed. For layer $k = 3$ there were 899 reflections, of which 806 were considered observed. The basis for accepting an intensity as statistically nonzero was the value of $\Delta I/I \leqslant 0.5$, where

$$\Delta I/I = (T + t^2 B)^{1/2}/(T - tB).$$

T equals total counts in time t_T for the ω scan, B = total background counts, t_1 and t_2 are background counting times, and $t = t_T/(t_1 + t_2)$. The intensities were converted to structure factor amplitudes by applying Lorentz and polarization corrections. No absorption corrections were made ($\mu_l = 129$ cm^{-1}). The equation

$$\sigma(F) = [(F/2I)^2(I + Bt/2 + 0.0004I^2)]^{1/2}$$

was used to estimate the variances for the structure factors, F. The values $1/\sigma^2(F)$ were used as weights in the least-squares calculation. A separate scale factor was used for $F(h0l)$ in the refinement.

$Ba_4Fe_2S_6[S_{1-y}(S_2)_y]$

The X-ray diffraction patterns of every crystal selected from the reaction product displayed the same twinning phenomenon. A parallelepiped-shaped crystal of dimensions 0.24 × 0.20 × 0.07 mm was selected for X-ray examination. Lattice constants at room temperature were obtained from a least-squares refinement of precise 2θ measurements of 40 reflections between 23° and 64° from the crystal mounted on a quarter circle diffractometer with the instrument set at a 1° take-off angle and 0.05° receiving aperture and using Mo radiation $\lambda_1 = 0.70926$ Å and $\lambda_2 = 0.71354$ Å. The results are given in Table I. The cell orientation is maintained as in the Al compound and the transformation matrices are identical. Three-dimensional X-ray diffraction intensity data to $(\sin\theta)/\lambda = 0.65$ and excluding layers $k = 1$, 2 were

measured with Mo$K\alpha$ radiation using a stationary crystal–stationary counter technique and balanced filters (*3*). A total of 2220 independent reflections was measured, and 1682 were regarded as observed on the basis that the peak count exceeded the background count by at least one standard deviation. The measured intensities were transformed into structure factor amplitudes after Lorentz, polarization, and absorption corrections were applied (transmission factors 0.352–0.691, $\mu_l = 142\ \text{cm}^{-1}$).

Reflections of equal intensity were observed from both compounds after a 180° rotation around the *b* axis so that twinning must be either by a two-fold rotation parallel to *b* or a mirror reflection perpendicular to *b*. The 2/*m* symmetry of reciprocal space implies equal volume for each twin. A further discussion of the twinning is presented later.

Structure Determination

$Ba_3(Ba_{0.6}Al_{0.4})Fe_2S_6[S_{0.6}(S_2)_{0.4}]$

The direct method for the determination of phases was used in the solution of the structure. A Wilson plot was obtained using all the data, and the statistics indicated that the crystal was centric. The computer programs FAME (by R. B. K. Dewar) and MULTAN (by P. Main, M. Woolfson, and G. Germain) were used to generate approximately 483 phases. A three-dimensional electron density map calculated with these phases showed three high peaks which were interpreted as barium atoms. Structure factors were calculated with these positions and a new map, produced from these phases, revealed eight peaks which were interpreted to represent 3 Ba, 2 Fe, and 3 S. Further calculations produced an electron density map from which 4 Ba, 2 Fe, and 7S were identified and it was also noticed that one of the Ba peaks was considerably lower than the others and remained lower throughout the calculations. A least-squares refinement with isotropic temperature factors and in which the occupancy factor of one Ba was fixed at 0.65 gave an *R* value of 0.14. The temperature factor of two of the sulfur atoms was also very large and this was taken as an indication that they did not have full occupancy. It was difficult to judge true peak heights and locations of the atoms with statistical occupancy factors because the omission of *h1l*, *h2l*, and *h3l* data produced strong diffraction ripples around these peaks. Indeed, the Al positions were found only after the careful comparison of the ripple structure around Ba(4) in the electron density maps calculated with and without *h3l*. Two small peaks were seen which were interpreted as Al. Least-squares refinement cycles in which temperature and occupancy factors were alternately kept constant finally yielded the parameters of Table II. The full-matrix least-squares program XFLS, a modification of ORFLS (by W. R. Busing, H. A. Levy, and K. O. Martin) was used. The function minimized was $\sum w(\text{KF}_0 - F_c)^2$ with $w = 1/\sigma^2$. The atomic scattering factors for Ba, Fe, Al, and S were those published in the International Tables and were corrected for the real part of dispersion effects. Anisotropic temperature factors were used for all the atoms except the aluminum and the disordered sulfur atoms. Final *R* is 0.072 for all observed reflections, excluding layer $k = 3$, and $wR = 0.086$,

$$\{R = \sum ||F_0| - |F_c||/\sum |F_0|$$
$$wR = [\sum w(F_0 - F_c)^2/\sum wF^2]^{1/2}\}.$$

For all reflections, excluding layer $k = 3$, the final *R* is 0.093 and $wR = 0.082$.[1] The final atomic parameters are shown in Table II. A three-dimensional difference electron density function was calculated with the last set of parameters, and no physically significant peaks were observed.

$Ba_4Fe_2S_6[S_{2/3}(S_2)_{1/3}]$

The positions of 3 Ba, 2 Fe, and 6 nondisordered S atoms from the previous structure were used as initial positions in the refinement of this structure. A three-dimensional electron density map indicated the position of a fourth Ba atom with full occupancy and three additional S atoms. Subsequent refinements with anisotropic temperature factors gave the positions and occupancies shown in Table III. A three-dimensional difference electron density map was calcu-

TABLE II

FINAL ATOMIC PARAMETERS[a] AND THEIR STANDARD DEVIATIONS ($\times 10^4$)[b] FOR $Ba_3(Ba_{0.6}Al_{0.4})Fe_2S_6[S_{0.6}(S_2)_{0.4}]$

Atom	x	y	z	β_{11}	β_{22}	β_{33}	β_{12}	β_{13}	β_{23}
Ba (1)	8016 (1)	9970 (1)	426 (0)	43 (1)	64 (3)	5 (0)	7 (1)	5 (0)	5 (0)
Ba (2)	2276 (1)	4991 (1)	898 (0)	38 (1)	64 (3)	7 (0)	−2 (1)	6 (0)	−1 (0)
Ba (3)	9203 (1)	4916 (1)	1970 (0)	52 (1)	60 (3)	5 (0)	7 (1)	6 (0)	4 (0)
Ba (4)[c]	5414 (2)	9969 (2)	1903 (1)	16 (1)	110 (3)	7 (0)	−10 (1)	4 (0)	0 (0)
Fe (1)	1295 (3)	9927 (2)	1640 (1)	50 (3)	58 (3)	7 (0)	2 (2)	7 (1)	1 (1)
Fe (2)	6157 (3)	4750 (3)	512 (1)	29 (2)	86 (3)	12 (0)	5 (2)	3 (1)	18 (1)
S (1)	1662 (5)	9 (4)	767 (2)	62 (5)	84 (5)	6 (1)	−4 (3)	10 (1)	−1 (1)
S (2)	8673 (4)	5034 (4)	551 (2)	31 (4)	75 (5)	8 (1)	−6 (3)	5 (1)	−2 (1)
S (3)	2451 (4)	2596 (3)	2103 (2)	56 (4)	31 (4)	8 (1)	−5 (2)	4 (1)	−4 (1)
S (4)	2546 (5)	7370 (3)	2077 (2)	65 (5)	40 (4)	10 (1)	8 (3)	4 (1)	8 (1)
S (5)	8832 (4)	9780 (4)	1709 (2)	45 (4)	95 (5)	6 (1)	−7 (3)	10 (1)	−1 (1)
S (6)	4858 (5)	7472 (4)	206 (3)	58 (5)	37 (5)	38 (2)	15 (3)	−20 (2)	−7 (2)
Atom	x	y	z	B	Occupancy				
S (7)	5714 (14)	4589 (12)	1404 (5)	3.50 (15)	0.6				
S (8)	5760 (20)	3438 (17)	1246 (7)	3.25 (21)	0.4				
S (9)	5413 (18)	4953 (14)	1896 (7)	2.68 (17)	0.4				
Al (1)	5407 (12)	1937 (9)	1889 (4)	1.0	0.50 (1)				
Al (2)	5418 (12)	7970 (9)	1888 (4)	1.0	0.50 (1)				

[a] The temperature factor is exp. $[-(\beta_{11}h^2 + \beta_{22}k^2 + \beta_{33}l^2 + 2\beta_{12}hk + 2\beta_{13}hl + 2\beta_{23}kl)]$.
[b] Except for B and occupancy.
[c] Occupancy set to 0.60.

TABLE III

FINAL ATOMIC PARAMETER[a] AND THEIR STANDARD DEVIATIONS ($\times 10^4$) FOR $Ba_4Fe_2S_6[S_{2/3}(S_2)_{1/3}]$

Atom	x	y	z	β_{11}	β_{22}	β_{33}	β_{12}	β_{13}	β_{23}
Ba (1)	8003 (1)	9955 (2)	426 (0)	38 (2)	105 (3)	4 (0)	6 (2)	2 (0)	7 (1)
Ba (2)	2246 (1)	5026 (2)	896 (1)	33 (2)	111 (3)	7 (0)	0 (2)	4 (1)	2 (1)
Ba (3)	9192 (1)	4932 (2)	1973 (1)	51 (2)	106 (3)	5 (0)	3 (2)	5 (1)	4 (1)
Ba (4)	5397 (2)	9937 (2)	1896 (1)	41 (2)	193 (4)	16 (0)	−7 (2)	7 (1)	6 (1)
Fe (1)	1271 (3)	9962 (4)	1635 (1)	40 (4)	100 (6)	4 (0)	0 (4)	6 (1)	1 (1)
Fe (2)	6136 (3)	4737 (5)	497 (1)	26 (4)	134 (7)	16 (1)	4 (4)	2 (1)	24 (2)
S (1)	1617 (6)	9973 (8)	762 (2)	55 (7)	152 (11)	3 (1)	6 (7)	5 (2)	3 (2)
S (2)	8628 (6)	5021 (7)	557 (2)	16 (6)	125 (10)	6 (1)	2 (6)	−3 (2)	5 (2)
S (3)	2459 (7)	2649 (8)	2094 (2)	56 (8)	131 (12)	9 (1)	−11 (8)	7 (2)	−7 (3)
S (4)	2522 (7)	7411 (8)	2090 (2)	59 (8)	129 (12)	8 (1)	4 (7)	7 (2)	8 (2)
S (5)	8830 (6)	9862 (7)	1714 (2)	30 (6)	150 (11)	4 (1)	3 (7)	5 (2)	2 (2)
S (6)	4852 (8)	7509 (9)	233 (4)	46 (9)	92 (13)	45 (3)	5 (8)	−14 (4)	−1 (4)
S (7)[b]	5708 (17)	4254 (39)	1350 (6)	29 (14)	759 (96)	12 (3)	−44 (31)	2 (6)	67 (15)
S (8)[c]	5288 (33)	2789 (44)	1034 (12)	154 (47)	351 (79)	28 (7)	157 (52)	27 (16)	66 (20)
S (9)[c]	5672 (39)	4598 (42)	1625 (15)	104 (42)	188 (56)	34 (11)	−10 (36)	1 (20)	5 (20)

[a] The temperature factor is exp. $[-(\beta_{11}h^2 + \beta_{22}k^2 + \beta_{33}l^2 + 2\beta_{12}hk + 2\beta_{13}hl + 2\beta_{23}kl)]$.
[b] Occupancy equals $\frac{2}{3}$.
[c] Occupancy equals $\frac{1}{3}$.

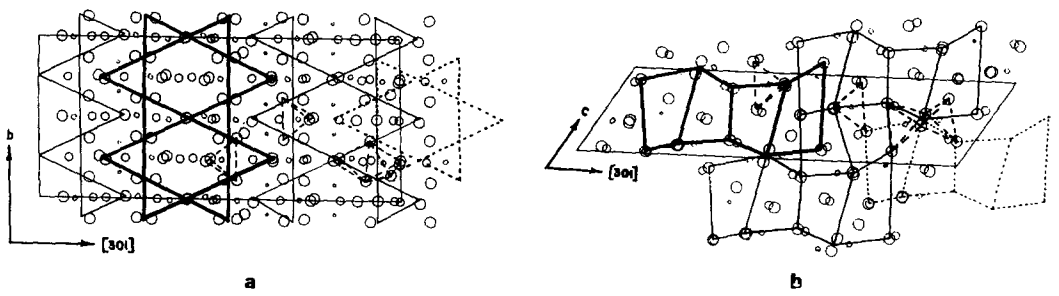

FIG. 1. Approximately mutually perpendicular projections of the crystal structure along the (a) $d(10\bar{3})$ vector and (b) $-b^*$. The largest circles represent S atoms, Ba atoms are the second largest, Fe atoms are third largest, and Al atoms are the smallest. The box in (a) 0–2 along b, and 0–1 along [301], and in (b) 0–1 along [301], and 0–½ along c.

lated with the last set of parameters, and no physically significant peaks were observed. The final $R = 0.053$, $wR = 0.047$ for observed reflections, and $R = 0.089$, $wR = 0.048$ for all reflections.[1]

The stoichiometry indicated by the refinement is $Ba_4Fe_2S_6[S_{2/3}(S_2)_{1/3}]$, a slightly lower S_2 concentration than in the previous structure. The minor variations may be due to slightly different reaction conditions of temperature and sulfur pressure.

Discussion of the Structure

Figure 1 shows two nearly mutually perpendicular projections and Fig. 2 is a stereoscopic view of the Al-containing phase. Distorted trigonal prisms of BaS_6 share edges to form hexagonal rings as in Ba_3FeS_5 and $Ba_{15}Fe_7S_{25}$ (*3*); however, two of the six trigonal prisms in the ring share only two edges leaving free lateral edges. The articulation of the rings by edge sharing forms a linear chain rather than a two-dimensional network as in the other two structures. The atomic occupancies inside the rings are almost identical to Ba_3FeS_5, with isolated FeS_4 tetrahedra and BaS_8 distorted cubes. Since the trigonal prisms do not share opposite triangular faces with identical rings the coordination of the Ba inside the ring is slightly different. The stacking of the rings is effected by sharing an edge of triangular faces of adjacent unique prisms, and the free lateral edges pointing in opposite directions. This type of articulation gives rise to a stairstep arrangement in which each hexagonal ring is shifted from the one below by one ring

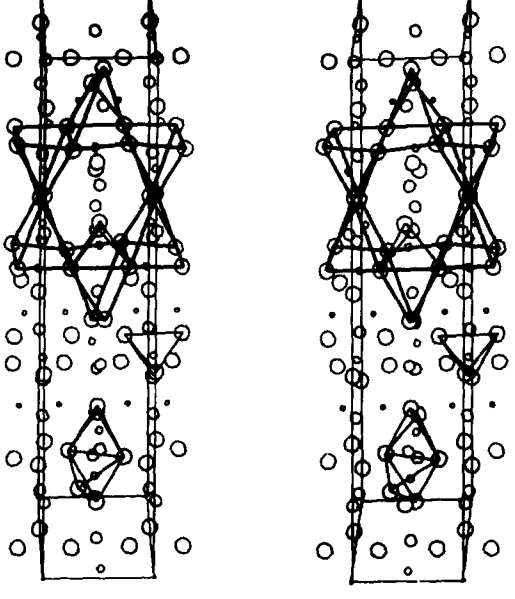

FIG. 2. Stereoscopic view of the crystal structure The box outlines 0–1 along the vertical [301], 0–1 along the horizontal b, and 0–½ along c.

[1] See NAPS Document No. 02963 for 30 pages of supplementary material. Order from ASIS/NAPS c/o Microfiche Publications, 440 Park Avenue South, New York, N.Y. 10016. Remit in advance for each NAPS accession number. Make check payable to "Microfiche Publications." Photocopies are $7.50. Microfiche are $3.00 each. Outside of the United States and Canada, postage is $3.00 for photocopy or $1.00 for a fiche.

diameter along the [301] direction. In Fig. 1 those successive levels are indicated. Adjacent stairstep units are displaced by one-half of the prism height along the ring axis. Thus a sulfur from the unshared edge of one chain is capping three rectangular faces of the prisms of the adjacent chain. This type of offset of trigonal prisms is fairly common (7). The interweaving of adjacent chains produces additional prisms which serve to link them together by sharing of trigonal faces, producing columns consisting of three prisms. At each terminal triangular face of the column is a Fe_2S_6 tetrahedral binuclear unit.

The Ba–Al disorder occurs at the trigonal prisms which have free edges in the hexagonal rings. When an Al atom replaces a Ba atom, it does not occupy the center of the trigonal prism, but instead, it moves into one of the two free square faces and occupies each on a statistical basis (see Fig. 3). Thus the Al atoms are close to two sulfur atoms of the face and to one sulfur which caps that face. This configuration and the values of the S–Al–S angles suggest a tetrahedral coordination of Al, with an electron in the 4th position, i.e., a hole–electron pair. On this basis the Ba^{+2} ion has been replaced by an $(Al - e)^{+2}$ unit. The charge balance is maintained by the reduction of the Fe atoms.

The important interatomic distances and angles are given in Tables IV and V where the estimated standard deviations are those from the least-squares refinement of the structures. In these compounds there are two crystallographically independent Fe–S tetrahedra. One is isolated and is located inside the ring. The other shares one edge with a centrosymmetrically related tetrahedron, thus forming an isolated binuclear unit. A sulfur atom which is part of the unshared edge, caps the rectangular faces, and is also part of the binuclear unit, is replaced on a statistical basis by S_2. Charge neutrality is maintained since $(S_2)^{2-}$ replaces S^{2-}. S–S distances are approximately 3.64 Å in both structures and correspond closely to the sum of the ionic radii. All sulfur atoms except S(9), which is part of the disulfide, are bonded to an iron atom and thus form the tetrahedra around these atoms. The iron–iron distances across the shared edge are 2.79 Å in the Ba–Fe–S compound and 2.86 Å in the Al substituted one. The nonbonding iron–iron distances are approximately 5.8 Å. The average Ba–S distance is about 3.3 Å.

The structural results obtained from the two compounds lead us to suggest that two types of disorder are present. In $Ba_4Fe_2S_6S_{2/3}(S_2)_{1/3}$ the end members of the crystal structures can be represented by the formulas $Ba_4Fe_2S_7$ and $Ba_4Fe_2S_6(S_2)$. When the disulfide ion, formed by S(8)–S(9), is present, then S(7) is always absent and vice versa. The trigonal prismatic environment around Ba(4) is irregular and has a trapezoidal shape. A nearly rectangular face is formed by S(3)–S(4)–S(4)–S(3)–S(3) with distances 3.24, 4.37, 3.24, and 4.50 Å, respectively. The edge of the "prism" is formed by S(1)–S(5) and is about 6.3 Å. Two S(7) are perpendicular to the prism edge and are 6.71 Å apart, the *b* axis dimension. Thus the polyhedron around Ba(4) could also be described as a distorted square antiprism formed by S(3)–S(4)–S(4)–S(3)–S(3) and S(1)–S(7)–S(5)–S(7)–S(1). The S(7) is easily replaced by S(8)–S(9) and it is suggested that the extent of this replacement is a function of temperature and sulfur vapor activity during the reaction. The latter is probably the more important parameter. The refinement of the Al free structure indi-

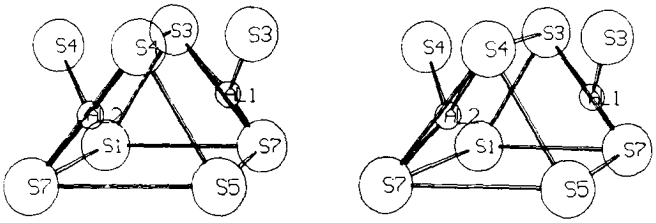

FIG. 3. Stereoscopic view of the vicinity of the Ba(4) trigonal prism showing the Al replacement.

TABLE IV

BOND DISTANCES AND ANGLES IN
$Ba_3(Ba_{0.6}Al_{0.4})Fe_2S_6[S_{0.6}(S_2)_{0.4}]$

	Distances (Å)		
Ba (1)–S (1)	3.034 (4)	Ba (2)–S (1)	3.464 (3)
Ba (1)–S (1)	3.167 (4)	Ba (2)–S (1)	3.410 (3)
Ba (1)–S (2)	3.469 (2)	Ba (2)–S (2)	3.132 (4)
Ba (1)–S (2)	3.414 (2)	Ba (2)–S (2)	3.458 (4)
Ba (1)–S (5)	3.070 (4)	Ba (2)–S (3)	3.386 (3)
Ba (1)–S (6)	3.201 (4)	Ba (2)–S (4)	3.252 (3)
Ba (1)–S (6)	3.206 (4)	Ba (2)–S (6)	3.633 (4)
		Ba (2)–S (7)	3.037 (13)
Ba (3)–S (2)	3.416 (4)	Ba (2)–S (8)	3.225 (17)
Ba (3)–S (3)	3.284 (3)	Ba (2)–S (9)	3.228 (16)
Ba (3)–S (3)	3.494 (3)		
Ba (3)–S (4)	3.361 (3)		
Ba (3)–S (4)	3.640 (3)	Ba (4)–S (3)	3.364 (3)
Ba (3)–S (5)	3.378 (3)	Ba (4)–S (3)	3.122 (3)
Ba (3)–S (5)	3.525 (3)	Ba (4)–S (4)	3.175 (4)
Ba (3)–S (5)	3.284 (4)	Ba (4)–S (4)	3.226 (3)
Ba (3)–S (7)	3.089 (13)	Ba (4)–S (5)	3.235 (4)
Ba (3)–S (8)	3.279 (17)	Ba (4)–S (7)	3.420 (9)
Ba (3)–S (9)	3.367 (16)		
		Ba (4)–S (8)	2.941 (13)
Fe (2)–S (2)	2.245 (4)	Ba (4)–S (9)	3.380 (9)
Fe (2)–S (6)	2.238 (4)	Ba (4)–S (9)	3.401 (9)
Fe (2)–S (6)	2.294 (4)	Ba (4)–S (9)	3.242 (16)
Fe (2)–S (7)	2.343 (13)		
Fe (2)–S (8)	2.142 (16)	Fe (1)–S (1)	2.267 (5)
Fe (2)–Fe (2)	2.859 (4)	Fe (1)–S (3)	2.215 (3)
		Fe (1)–S (5)	2.223 (3)
		Fe (1)–S (5)	2.267 (4)
S (8)–S (9)	1.986 (20)		
Al (1)–S (3)	2.74 (1)	Al (2)–S (4)	2.75 (1)
Al (1)–S (3)	2.88 (1)	Al (2)–S (4)	2.77 (1)
Al (1)–S (7)	2.24 (1)	Al (2)–S (7)	2.62 (1)
	Angles (degrees)		
S (5)–Fe (1)–S (4)	108.7 (1)	S (7)–Fe (2)–S (6)	123.8 (3)
S (5)–Fe (1)–S (3)	108.8 (1)	S (7)–Fe (2)–S (6)	99.7 (3)
S (5)–Fe (1)–S (1)	117.4 (2)	S (7)–Fe (2)–S (2)	112.3 (3)
S (4)–Fe (1)–S (3)	106.1 (1)	S (6)–Fe (2)–S (6)	101.8 (2)
S (4)–Fe (1)–S (1)	108.3 (1)	S (6)–Fe (2)–S (2)	105.7 (2)
S (3)–Fe (1)–S (1)	107.1 (1)	S (6)–Fe (2)–S (2)	112.8 (1)
		S (8)–Fe (2)–S (6)	117.3 (4)
		S (8)–Fe (2)–S (6)	105.1 (4)
		S (8)–Fe (2)–S (2)	112.4 (5)
S (3)–Al (1)–S (7)	102.2 (4)	S (4)–Al (2)–S (7)	99.8 (4)
S (3)–Al (1)–S (3)	106.5 (3)	S (4)–Al (2)–S (4)	104.7 (4)
S (3)–Al (1)–S (7)	105.1 (4)	S (4)–Al (2)–S (7)	101.8 (4)

TABLE V

BOND DISTANCES AND ANGLES IN $Ba_4Fe_2S_6[S_{2/3}(S_2)_{1/3}]$

	Distances (Å)		
Ba (1)–S (1)	3.142 (5)	Ba (2)–S (1)	3.383 (5)
Ba (1)–S (1)	3.039 (4)	Ba (2)–S (1)	3.423 (5)
Ba (1)–S (2)	3.432 (4)	Ba (2)–S (2)	3.145 (5)
Ba (1)–S (2)	3.375 (4)	Ba (2)–S (2)	3.461 (4)
Ba (1)–S (5)	3.070 (4)	Ba (2)–S (3)	3.356 (5)
Ba (1)–S (6)	3.178 (6)	Ba (2)–S (4)	3.265 (5)
Ba (1)–S (6)	3.198 (6)	Ba (2)–S (6)	3.604 (6)
		Ba (2)–S (7)	3.081 (13)
		Ba (2)–S (8)	3.085 (26)
		Ba (2)–S (9)	3.159 (31)
Ba (3)–S (2)	3.398 (4)		
Ba (3)–S (3)	3.282 (5)		
Ba (3)–S (3)	3.526 (5)	Ba (4)–S (3)	3.362 (5)
Ba (3)–S (4)	3.352 (5)	Ba (4)–S (3)	3.126 (5)
Ba (3)–S (4)	3.551 (5)	Ba (4)–S (4)	3.222 (5)
Ba (3)–S (5)	3.390 (4)	Ba (4)–S (4)	3.176 (5)
Ba (3)–S (5)	3.439 (4)	Ba (4)–S (5)	3.238 (5)
Ba (3)–S (5)	3.263 (4)	Ba (4)–S (7)	3.266 (19)
Ba (3)–S (7)	3.132 (13)	Ba (4)–S (8)	2.877 (26)
Ba (3)–S (9)	3.065 (3)	Ba (4)–S (9)	3.233 (25)
		Ba (4)–S (9)	3.651 (25)
Fe (2)–S (2)	2.216 (5)	Fe (1)–S (1)	2.254 (5)
Fe (2)–S (6)	2.224 (6)	Fe (1)–S (3)	2.211 (5)
Fe (2)–S (6)	2.301 (7)	Fe (1)–S (4)	2.225 (5)
Fe (2)–S (7)	2.267 (12)	Fe (1)–S (5)	2.257 (5)
Fe (2)–S (8)	2.157 (26)		
Fe (2)–Fe (2)	2.787 (4)		
S (8)–S (9)	1.830 (39)		
	Angles (degrees)		
S (5)–Fe (1)–S (4)	108.5 (2)	S (7)–Fe (2)–S (6)	119.9 (5)
S (5)–Fe (1)–S (3)	108.8 (2)	S (7)–Fe (2)–S (6)	102.1 (5)
S (5)–Fe (1)–S (1)	117.6 (2)	S (7)–Fe (2)–S (2)	111.4 (4)
S (4)–Fe (1)–S (3)	104.8 (2)	S (6)–Fe (2)–S (6)	104.0 (3)
S (4)–Fe (1)–S (1)	109.0 (2)	S (6)–Fe (2)–S (2)	106.0 (2)
S (3)–Fe (1)–S (1)	107.4 (2)	S (6)–Fe (2)–S (2)	113.5 (2)
		S (8)–Fe (2)–S (6)	117.7 (7)
		S (8)–Fe (2)–S (6)	88.0 (7)
		S (8)–Fe (2)–S (2)	121.2 (7)

cates that $\frac{2}{3}$ of this specimen contained sulfide and $\frac{1}{3}$ the disulfide ion.

When Al was present in the reacting mixture Ba(4) is replaced in the manner described above. However, this replacement occurs only in the sulfide structure. The exclusion of Al in the disulfide structure is based on the fact that unrealistically short Al–S distances of about 2 Å would be present. The S–S distances shown in Tables IV and V and the occupancy factors are probably the least reliable results because of the forced omission of a large number of diffraction data and the strong correlations between the various parameters of statistical atoms. Table II shows a sum of occupancies for Ba and Al of 1.6

but on the basis of other evidence discussed below, we believe the approximate composition of this phase to be $[Ba_3AlFe_2S_7]_{0.4} \cdot [Ba_4Fe_2S_7]_{0.2} \cdot [Ba_4Fe_2S_6(S_2)]_{0.4}$.

Using the sum of the bond strengths [8] for Fe–S (nondisulfide) distances in $Ba_4Fe_2S_6[S_{2/3}(S_2)_{1/3}]$, charges on the iron in sites 1 and 2 are 2.97 and 2.85, respectively. For the aluminum substituted material these are 2.92 and 2.63, respectively, for an average of 2.77. These calculations indicate that the total aluminum concentration is approximately 0.4 and that the charge reduction occurs on the iron ion in the binuclear unit.

As stated earlier, the twinning in both structures was such that there was a pseudo-mirror perpendicular to the b axis of the *A*-centered cell or that there was a pseudo-twofold rotation axis parallel to the *b* axis. All the barium and iron atoms and most of the sulfur atoms are almost at positions x, 0, z. The other sulfur atoms and the aluminum atoms come in pairs at positions x, y, z; x, $\bar{y}$, z. Atom S(8) is the exception. This type of atomic arrangement suggests that a pseudo-mirror perpendicular to the *b* axis at $y = 0$ could be present with only small displacement of the heavy metal atoms and most of the sulfur atoms. The displacements for the mirroring or twofold rotation of the barium atoms and most other atoms are less than 0.1 Å. Therefore, the structure can switch from one twin to the other without major disruptions of the crystal and this occurs probably every few hundred or thousand unit cells.

Magnetic and Electrical Measurements

The results of the magnetic measurements on the aluminum substituted phase are shown in the form of $1/x_g$ versus temperature in Fig. 4. This compound exhibits incipient magnetic ordering near 120°K. The effective magnetic moment calculated from the linear portion of the curve is 5.33 BM and $\theta = -534$°K. Assuming a spin-only contribution to the effective moment, a net spin of approximately 2.25 results. This spin implies that the average charge on the iron would be +2.5 or an Al occupancy of 1.0. This lower moment

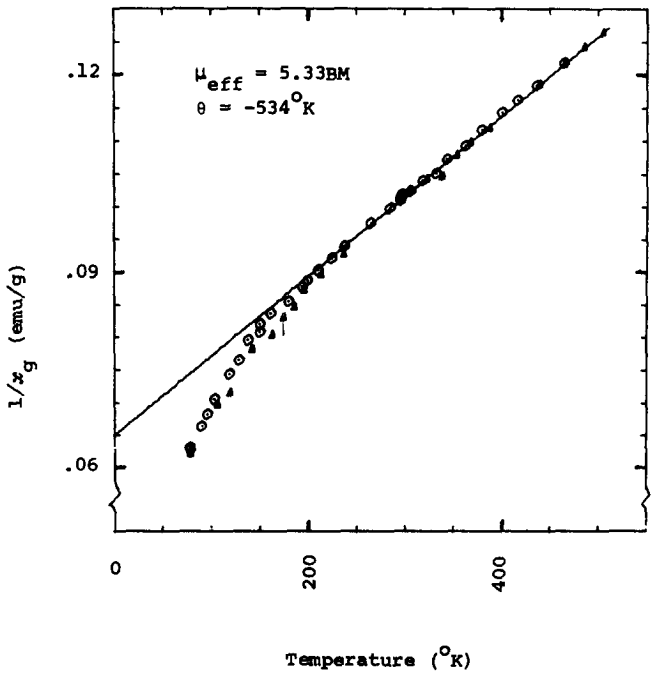

FIG. 4. Reciprocal magnetic susceptibility versus temperature for $Ba_3(Ba_{0.6}Al_{0.4})Fe_2S_6[S_{0.6}(S_2)_{0.4}]$. Different symbols represent separate measurements.

is probably due to the presence of a small amount of nonmagnetic impurities such as BaS or Al_2S_3.

The electrical resistivity of the Ba–Fe–S material was measured at room temperature on a crystal ~0.1 mm on each edge. The result was a fairly high value of about 10^5 ohm-cm as expected since a continuous chain of edge sharing Fe–S tetrahedra is not present in this structure.

Mössbauer Spectra

The structure consists of isolated FeS_4 tetrahedra and isolated Fe_2S_6 dimers formed by edge-sharing tetrahedra. The spectrum, Fig. 5a, indicates two types of iron atoms with isomer shifts of 0.20 mm/sec relative to α-Fe and quadrupole splittings of about 0.45 and 0.90 mm/sec. This value of the isomer shift indicates a charge of 3.0 on the iron atoms, with the iron in the isolated tetrahedra having the smaller quadrupole splitting. However, the spectrum from the aluminum substituted compound, Fig. 5b, is much more complicated and assigning isomer shifts and quadrupole splittings to a definite site was not possible. The larger quadrupole splitting and overall isomer shift of 0.30 mm/sec is indicative of an average charge on the iron atoms of about

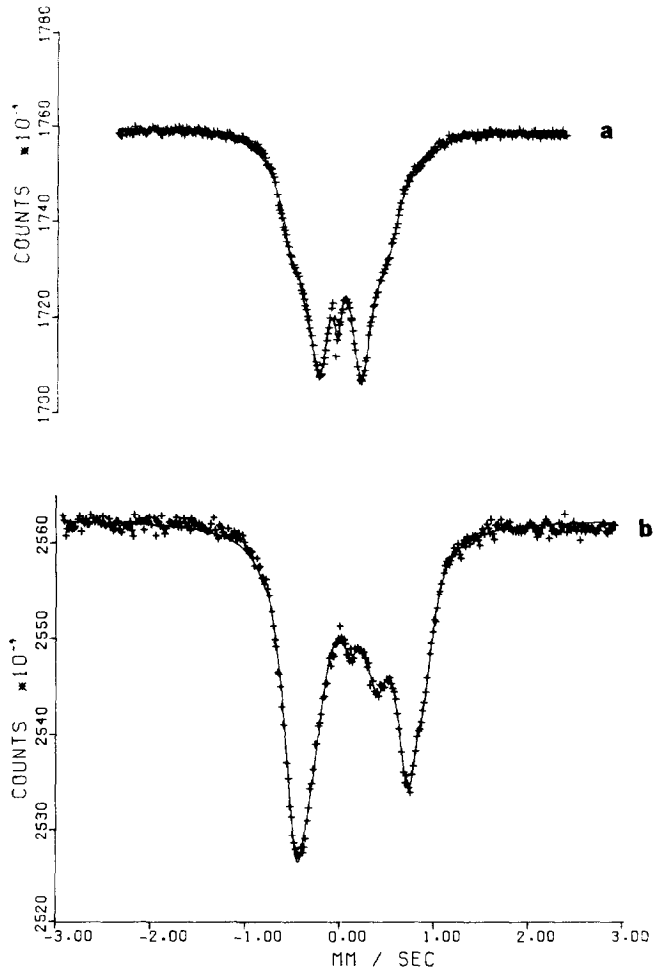

FIG. 5. Mössbauer spectra at 22°C of (a) $Ba_4Fe_2S_6[S_{2/3}(S_2)_{1/3}]$ and (b) $Ba_3(Ba_{0.6}Al_{0.4})Fe_2S_6[S_{0.6}(S_2)_{0.4}]$. The lines represent least-squares calculated spectra assuming Lorentzian line shapes.

2.75. This implies a total aluminum occupancy of approximately 0.5.

The small peaks at the center of each spectrum seem to be an artifact of the spectra. These may be a result of the collapse of the spectra into a single line due to very small particle size in the absorber material produced by the polytypic twinning.

Summary

The crystal structure refinements indicate that the occupancy of Ba(4) was 0.60 and the Al occupancy was ~1.00. However, due to the partial data set, disorder, and relatively light atoms, the occupancy factors of the Al atoms are subject to large errors. Better indications of the true value of the Al occupancy is the Mössbauer isomer shift for the iron, the value of the Ba(4) occupancy, chemical analysis, and calculated iron valencies. These all indicate that the Al occupancy is approximately 0.4 to 0.5. Al does not substitute for Fe in the tetrahedral sites. It replaces Ba but not within the trigonal prism of S ions. Instead it is located statistically on each side of a rectangular prism face and has only three nearest-neighbor sulfide ions.

Acknowledgments

The authors gratefully acknowledge the research support provided by grants from the Robert A. Welch Foundation, Houston, Texas, and the National Science Foundation. We thank Professor R. L. Collins, Department of Physics, The University of Texas at Austin for permitting us to use his Mössbauer equipment and for the many helpful discussions concerning the interpretation of the data.

References

1. I. E. GREY, H. HONG, and H. STEINFINK, *Inorg. Chem.* **10**, 340 (1971).
2. H. HONG AND H. STEINFINK, *J. Solid State Chem.* **5**, 93 (1972).
3. J. T. LEMLEY, J. M. JENKS, J. T. HOGGINS, Z. ELIEZER, AND H. STEINFINK, *J. Solid State Chem.* **16**, 117 (1976).
4. J. T. HOGGINS AND H. STEINFINK, *Acta Cryst. B*, **33**, 673 (1977).
5. J. G. COSGROVE AND R. L. COLLINS, *Nucl. Inst. Meth.* **95**, 269 (1971).
6. L. F. BATES, "Modern Magnetism," 4th ed., p. 134, Cambridge Univ. Press, New York (1963).
7. C. B. SHOEMAKER, *Z. Krist.* **137**, 225 (1973); J. E. IGLESIAS AND H. STEINFINK, *Z. Krist.* **142**, 398 (1975).
8. J. T. HOGGINS AND H. STEINFINK, *Inorg. Chem.* **15**, 1682 (1976).